JOURNAL OF GEOPHYSICAL RESEARCH, VOL. 93, NO. A9, PAGES 9555–9567, SEPTEMBER 1, 1988

The Role of Interplanetary Shocks in the Longitude Distribution of Solar Energetic Particles

H. V. CANE,[1] D. V. REAMES, AND T. T. VON ROSENVINGE

Laboratory for High Energy Astrophysics, NASA Goddard Space Flight Center, Greenbelt, Maryland

A study of solar proton events with well-identified sources has been carried out using data from Goddard particle experiments on IMPs 4, 5, 7, and 8 and ISEE 3. The experiments cover the energy range from about 1 to 300 MeV. The 235 events of our study represent approximately 70% of all increases above 10^{-3} particles cm^{-2} sr^{-1} s^{-1} MeV^{-1} at energies > 20 MeV detected in a 19.7-year period commencing mid-May 1967. It is shown that intensity-time profiles of solar proton events display an organization with respect to heliolongitude. Whilst it has been known for many years that the profile of a proton event depends on the longitude of the solar event relative to the observer, we suggest that the major controlling agent is the existence of an interplanetary (IP) shock. Furthermore, we explain the change in shape as a function of heliolongitude within the framework of a recently derived model for the large-scale structure of IP shocks. In particular, the long delay to maximum intensity for far eastern events (a property previously ascribed to coronal processes) and the overall extended duration can be accounted for by IP shock acceleration and continued magnetic connection to the shock even after it has propagated beyond 1 AU.

1. INTRODUCTION

Extensive studies of solar energetic particles have been undertaken in the past. Two studies which have dealt with a large sample of events are those of *Reinhard and Wibberenz* [1974] and of *Van Hollebeke et al.* [1975]. The results of these and other studies have been interpreted to imply that particles propagate promptly when the source region is magnetically well connected to the observer. The solar longitude extent of the "fast propagation region" is usually in the range W10° to W90° but can extend from E30° to W140°. For prompt events the observed intensity profiles are often smooth and have a form (see Figure 1*a*) that can be modelled [e.g., *Parker*, 1963] using diffusive transport theory. Note, however, that questions have been raised as to the ability of diffusive transport theory alone to explain these profiles. The short durations of events associated with impulsive flares suggest that the longer durations of "normal" proton events result from sustained injection of particles, in addition to diffusion [*Cane et al.*, 1986; *Reames and Stone*, 1986]. Likewise, consideration of data for individual events has led workers to invoke extended injections [*Wibberenz et al.*, 1976; *Beeck et al.*, 1987].

The intensity profiles of solar proton events take different forms, with the most pronounced intensity changes being associated with interplanetary (IP) shocks, particularly at energies below 20 MeV. The low-energy particle enhancements associated with IP shocks are called Energetic Storm Particle (ESP) events [*Bryant et al.*, 1962]. The name arose because of the early recognition that IP shocks were responsible for rapid onsets of geomagnetic storms. The schematic intensity-time profile of Figure 1*b* shows a pronounced intensity peak at the passage of a shock which is superposed on the decay phase of a "normal diffusion" event, i.e., one with a profile like Figure 1*a*. Profiles of the form in Figure 1*b* are, in fact, rare. Nevertheless, many researchers think that the effects of IP shocks can be ignored when the particle intensities do not show an obvious enhancement at shock passage.

At low energies, less than a few hundred keV, particle enhancements are clearly associated with IP shocks. Considerable progress has been made recently in understanding the characteristics of ion acceleration at these energies. The low-energy ion experiment on ISEE 3 [*Sanderson et al.*, 1981] has provided a wealth of information about ion intensities and anisotropies in association with the shocks which have simultaneously been observed with plasma and magnetic field experiments. *Lee*'s [1983] theory for diffusive acceleration has been extensively tested [*Kennel et al.*, 1986] on a single event and found to predict many of the observed properties. However, the theory applies at energies below about 200 keV, and essentially all the recent work on shock acceleration has concentrated on the energy range of less than a few hundred keV.

Nevertheless, shock-associated enhancements are observed even at energies as high as 100 MeV, as we illustrate in this paper. We show that IP shocks play a crucial role in supplying particles to regions not magnetically connected to the source region. Most solar proton events are composed of a solar component, with its origins in the solar corona, and an interplanetary component, associated with an IP shock. Such an idea has previously been suggested by *Evenson et al.* [1982] on the basis of an analysis of two events. We argue that the interplanetary component is more important than most researchers have previously recognized. An initial report of our work has been presented [*Cane et al.*, 1987].

The separation of solar proton intensity profiles into two components is not as straightforward as suggested by Figure 1*b*. We suggest that the relative contribution of the two components is a function of (1) the heliolongitude of the source region, (2) the strength of the associated shock, and (3) the energy of the observations. In general, these factors result in characteristic profiles for different longitude ranges and different energies.

Few attempts have been made to model particle intensity profiles including prompt solar particles and the effects of shocks. The recent work of *Lee and Ryan* [1986] and the earlier work of *Scholer and Morfill* [1975] concentrated on modelling the effect of the shock as a function of shock speed

[1]Also at Department of Physics and Astronomy, University of Maryland, College Park.

Paper number 8A9498.
0148-0227/88/008A-9498$05.00

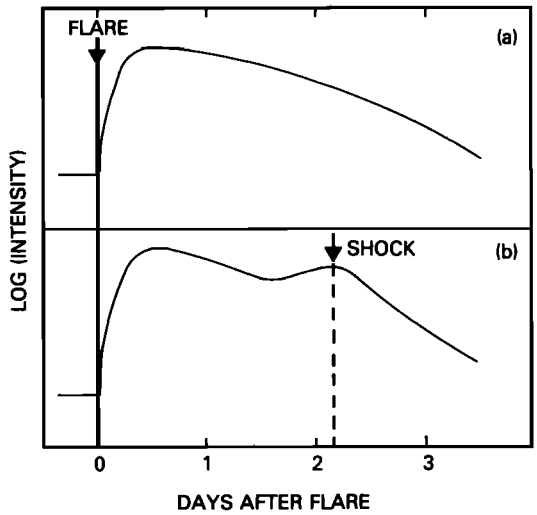

Fig. 1. Idealized schematic illustration of proton intensities measured at 1 AU following a western flare when a shock (*a*) is not and (*b*) is observed at Earth.

and of the interplanetary mean free path. The change in shock characteristics as a function of the field line connection of the observer to the shock has not been considered theoretically. We argue that this is very important, and in this paper we show that the variation of particle intensity profiles can be understood in terms of the large-scale structure of IP shocks.

2. Data Analysis

The study commenced by assembling a list of all proton events with intensity above 3×10^{-3} particles cm^{-2} sr^{-1} s^{-1} MeV^{-1} in the energy range 9–23 MeV for the period mid-May 1967 to the end of 1985. The source of data was Goddard Space Flight Center experiments on IMPs 4, 5, 7, and 8 and ISEE 3. The particle list for the study was the same as that used by *Cane* [1988], and a more detailed description of the source identifications can be found there. The source identifications for the majority of the particle events which occurred during this time period have been published previously (for the period 1967–1972, see *Van Hollebeke et al.* [1975], for the period mid-1973–1979, see *Kahler* [1982], and for the period mid-1978–1982 see *Cane et al.* [1986]. We began, however, by making flare associations without reference to these previous studies. The associations derived were essentially the same as those arrived at by earlier workers. The major difference was that a number of events with less confident associations and some of the smaller events from the *Van Hollebeke et al.* [1975] compilation were not included.

The final list comprises 235 proton events with well-identified sources. For 80% there were reported soft X ray, H α, and metric radio phenomena occurring close in time to the onset of the particles. In the *Cane* [1988] paper the particle events were used to generate a list of flare-associated interplanetary shocks. The important information obtained was the time the shock reached the earth, based on the sudden commencement (SC) of a geomagnetic storm, and the size of the SC. These properties are important for the present study. *Cane* [1988] has shown that the size of an SC is a good estimate of the strength (as given by the compression ratio) of the associated shock.

The distribution of the 235 events as a function of heliolongitude is shown in Figure 2. The cross-hatched histogram shows the events followed by IP shocks detected at earth as evidenced by an SC. This comprises the vast majority of events from eastern regions. Based on studies of the associations between soft X ray flares, IP shocks, and energetic protons [*Cane*, 1985, 1988 and references therein] it is probable that all the associated solar events from the far east resulted in IP shocks but some did not extend as far as the earth. A number of far eastern events for which shocks were not detected at Earth were associated with IP shocks as evidenced by IP type II emission [*Cane*, 1985]. The presence of shocks in nearly all poorly connected events is obviously a crucial factor. We now proceed to illustrate how the presence of shocks affects the observed intensity profiles. Our contention is that the various forms displayed by energetic solar proton events fall into a pattern if they are organized according to the heliolongitude of the source and consideration is taken of the presence and strength of associated IP shocks. Our deductions are based on an analysis of many events viewed from one location (the Earth) and are supported by observations of single events viewed from more than one location.

Figure 3 shows five events from well-connected source regions. At energies above 20 MeV these events have smooth profiles and have the form often described as being "diffusive," i.e., can be modelled using simple diffusive transport theory. Three of the events are associated with interplanetary shocks whose times of passage are indicated by dashed lines. The times of H α flare maxima are indicated by solid lines. The shock of April 26, 1981, was the strongest, with an estimated compression ratio (ratio of downstream to upstream density) of 3.1. The shocks of November 25, 1977, and July 23, 1981, were weaker and have estimated strengths of 2.3 and 2.0, respectively. These shocks could be responsible for the extended duration of enhanced intensities at low energies, but there is only a small effect near shock passage. Note that the model (which excluded IP shock acceleration) fitted to the November 1977 event by *Beeck et al.* [1987] did not describe the late phase of the event very well.

Figure 4 shows three more well-connected events and one that is not. The events of September 7, 1978, and November 26, 1982, were not associated with shocks at Earth and have smooth profiles. The events of April 3, 1979, and November

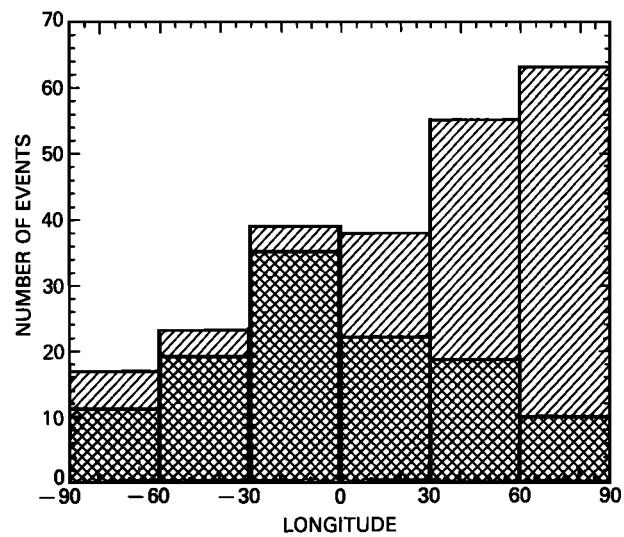

Fig. 2. Distribution with respect to heliolongitude of the 235 events which form the basis of this study. The cross-hatched histogram represents the events associated with shocks detected at Earth.

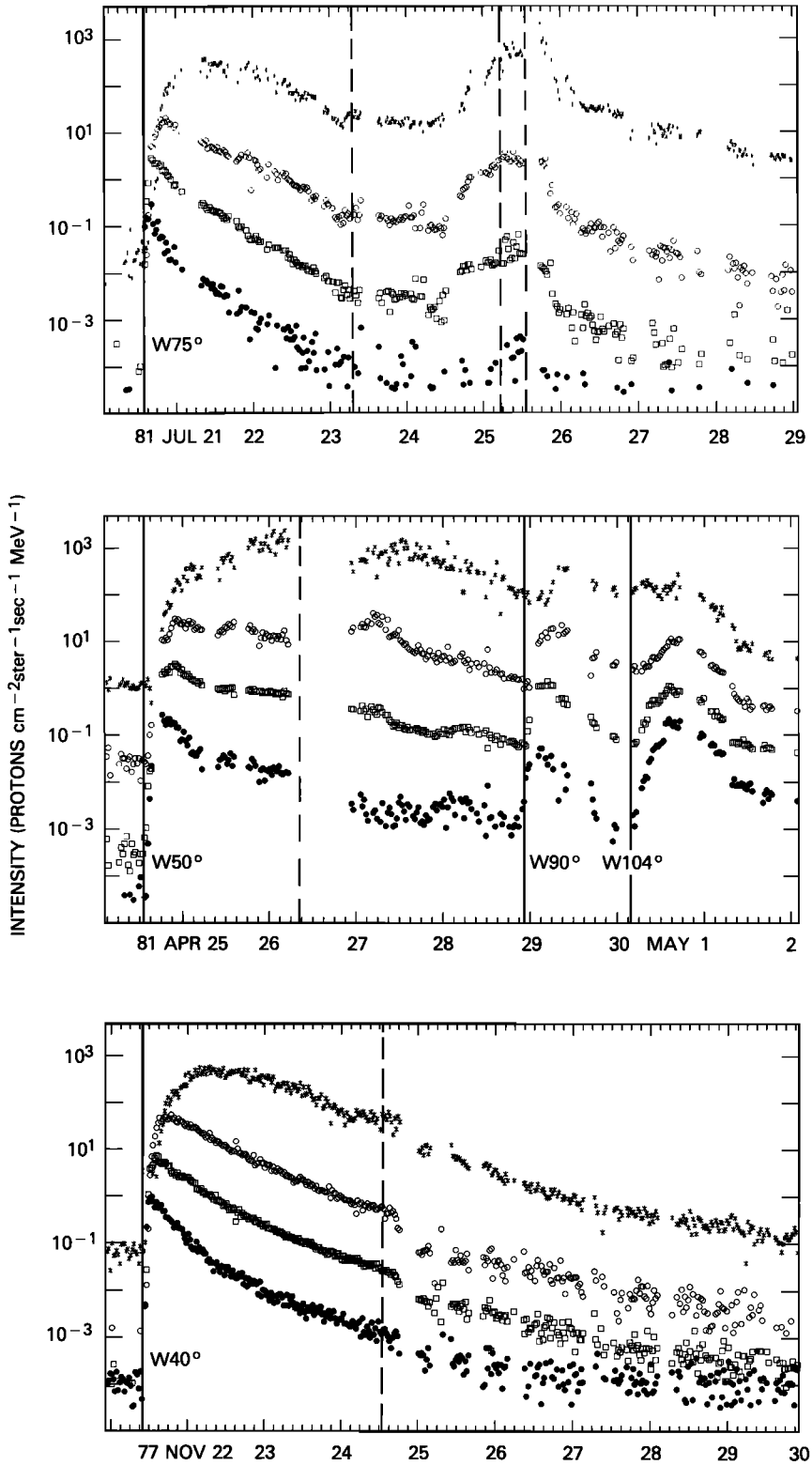

Fig. 3. Proton intensities observed at IMP 8 for four energy ranges, 1.8–2.3 (stars), 9–11 (open circles), 24–28 (open squares), and 63–81 (solid circles) MeV. Times of associated flares and their far western longitudes are indicated. Shock passages at Earth are indicated with dashed lines. The events are ordered, going from west to east, according to the longitudes of their sources.

22, 1982, are two of the few events which show an enhancement at shock passage superimposed on the decay phase of a "normal" event. Both these shocks were relatively strong, with estimated compression ratios of 2.3 and > 3.5, respectively.

The shocks originating between W10° and E45° are usually the strongest [*Cane*, 1988]. Sources from this region generate the highest shock-associated intensities, as may be seen in Figures 5 and 6. Note that in Figure 6 (bottom) one can imagine that at energies below 80 MeV the profile might well be the superposition of a solar and a shock component, with

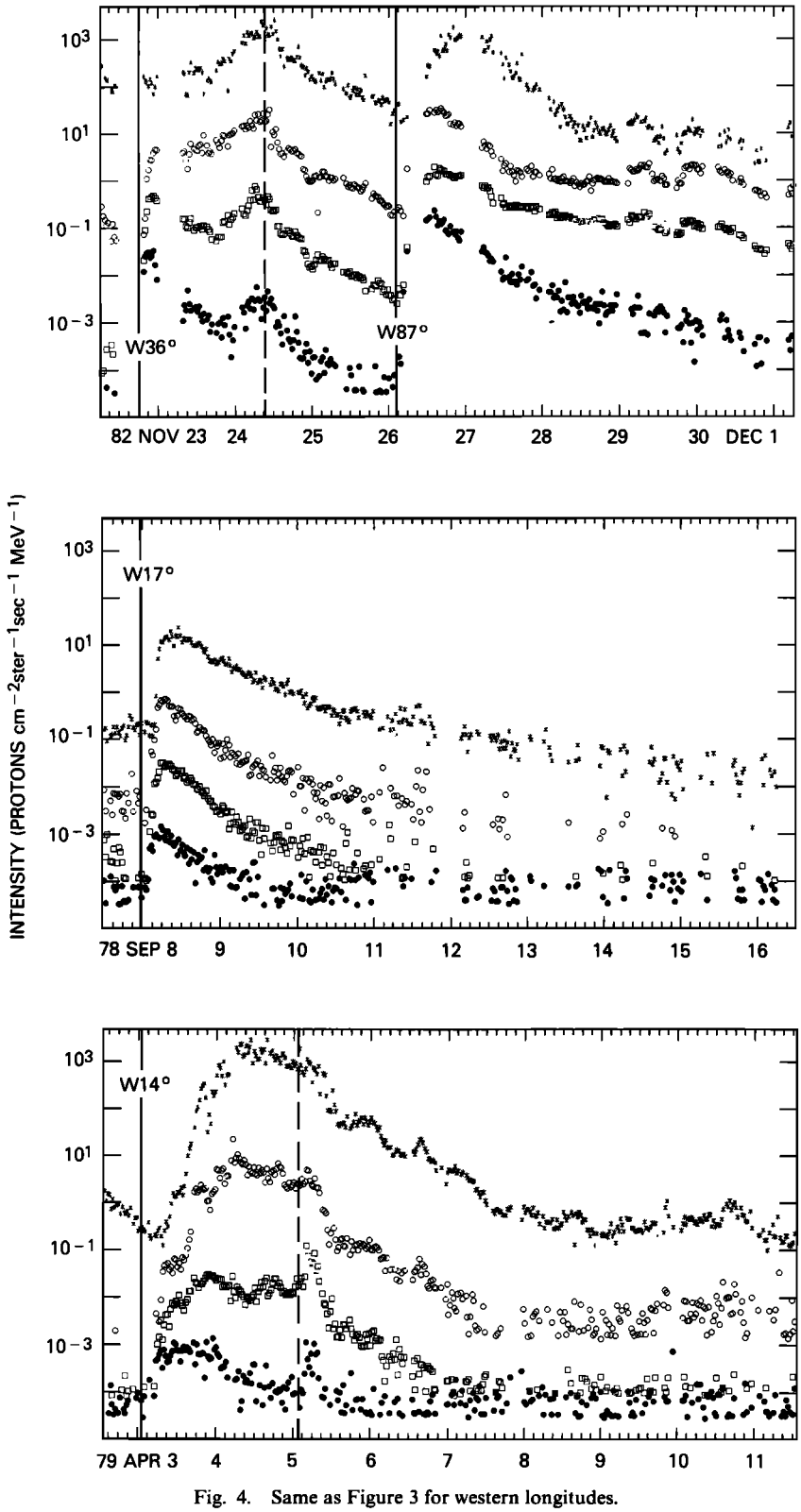

Fig. 4. Same as Figure 3 for western longitudes.

the solar component having the shape exhibited at the highest energies.

The January 3, 1978, November 12, 1978, and April 5, 1979, shocks (Figures 5 (bottom), 5 (center), and 4 (bottom), respectively) have been documented as being followed by drivers [*Burlaga et al.*, 1981; *Bame et al.*, 1981; *Gosling et al.*, 1987]. For these events a drop in intensity occurs when the spacecraft encounters the shock driver. This has previously been noted for the January 1978 event by *Richter et al.* [1981] and for other events at lower energies [e.g., *Sanderson et al.*, 1983]. Similarly, the profile in Figure 5 (top) suggests the presence of a driver.

The profiles in Figure 7 bear little resemblance to those in the earlier figures except for the above 80-MeV profile for the

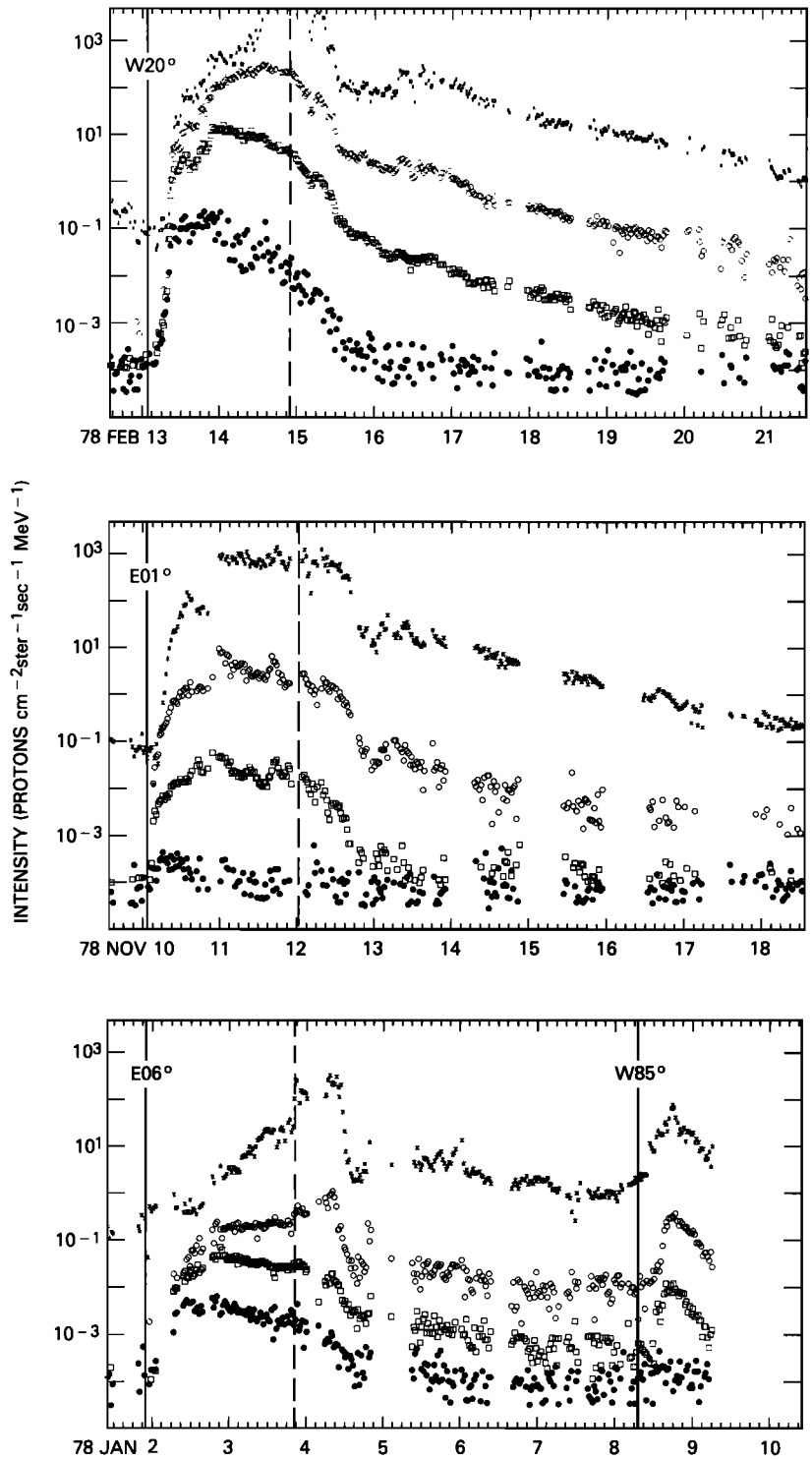

Fig. 5. Same as Figure 3 for longitudes near central meridian.

September 7, 1977, event. For far eastern events, peak intensities occur many days after the flare, frequently after the shock has passed (e.g., the February 1984 event in Figure 7 (center)). The December 1982 event (Figure 6 (center)) also peaked after the shock. For some far eastern events the shock does not extend as far as the Earth, but there is good evidence that the shocks exist.

In summary, then, the profiles change in appearance as a function of longitude. Events from further west than about W20° have relatively smooth profiles with a single maximum early in the event. The majority of these events are not associated with shocks. Those that are generally show little effect at shock passage. If the shock is strong, there can be enhancements at shock passage, but they are generally restricted to energies below 50 MeV.

For events originating within about 30° of central meridian the shock effects at energies below 20 MeV can be dramatic. After a large enhancement at shock passage (sometimes satu-

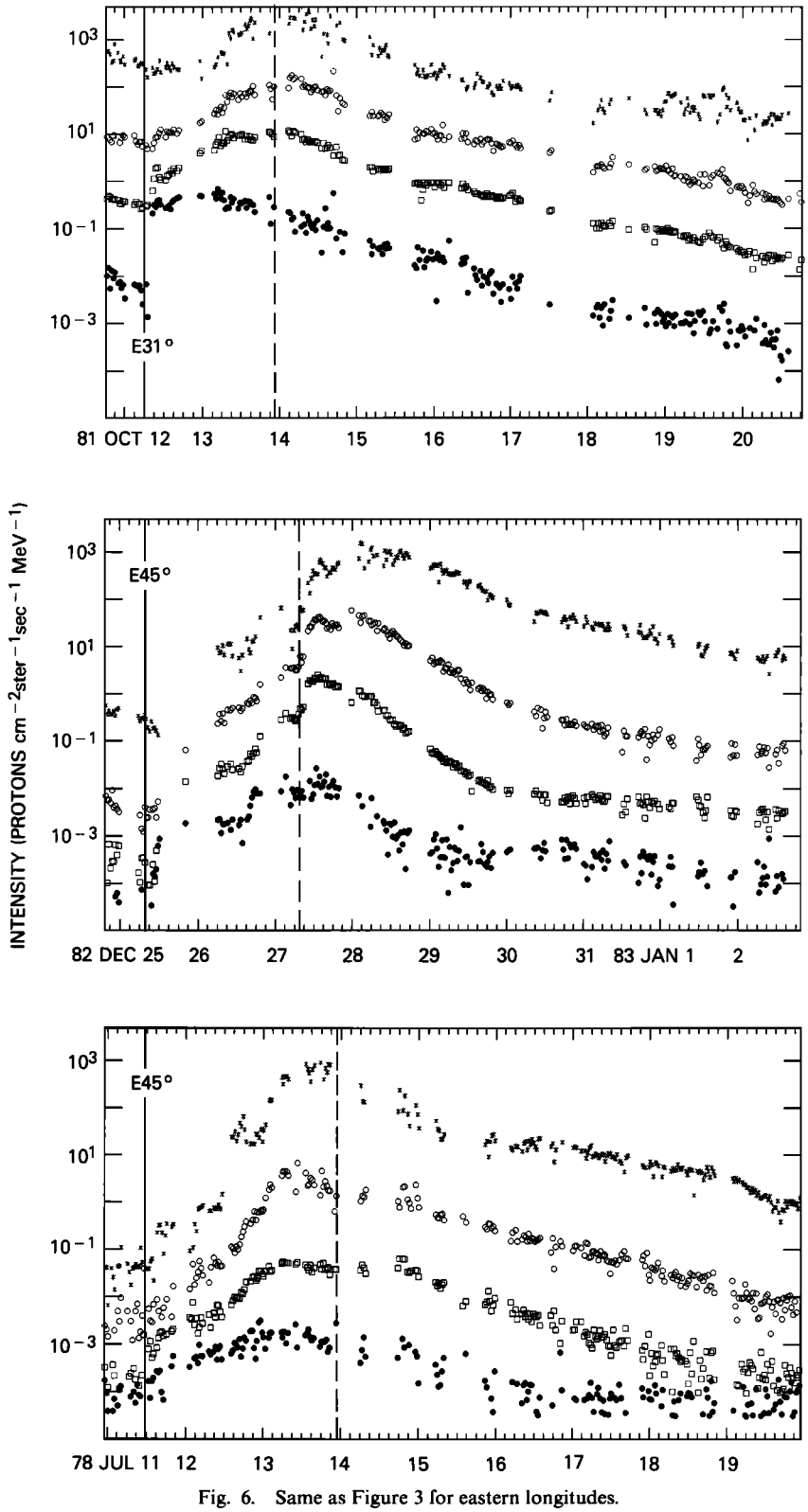

Fig. 6. Same as Figure 3 for eastern longitudes.

rating the detectors at energies near 1 MeV) the low-energy intensities often plummet by an order of magnitude or more.

Further east the events become very drawn out, with the east limb events lasting for more than 6 days at least up to 40 MeV and sometimes to even higher energies. For most of these events the highest intensities occur after the shock has passed.

We have performed a statistical analysis to illustrate that these properties are common to the majority of events. We summarized the complete list of events by recording peak intensities and time delays to peak intensities for each of six energy bands (three for IMPs 4 and 5). The delays were relative to the times of maximum H α emission of the associated flares. The energy bands were 1–2, 9–24, 24–43, 43–81, 93–121,

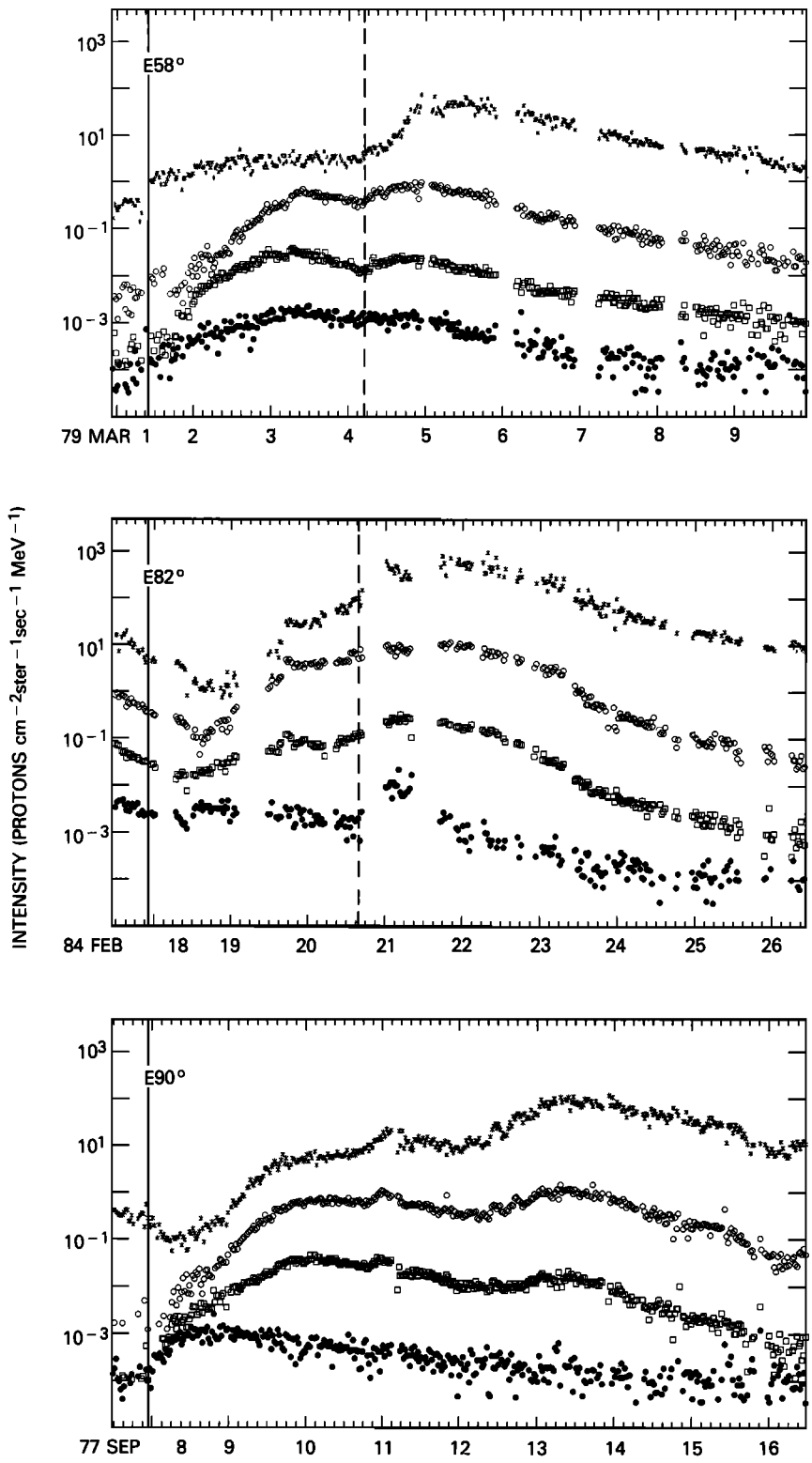

Fig. 7. Same as Figure 3 for far eastern longitudes.

and 121–327 MeV. Note that for this procedure, obvious shock effects (i.e., enhancements at shock passage) were included. We considered "an event" to include the whole period of enhanced intensity, even if it lasted many days, provided there was no obvious new solar injection of particles. (No peak was recorded if there was any confusion because of multiple events.) In some cases the peak results from solar particles, in other cases, from IP particles, and much of the time is a combination. Previously, researchers [e.g., *Sarris et al.*, 1984] have attempted to separate the solar and IP components, but we believe that it is not possible using intensity profiles alone. In future studies we intend to use composition and anisotropy data. Our procedure avoids a priori assumptions about the relative contributions of the components. We investigate the

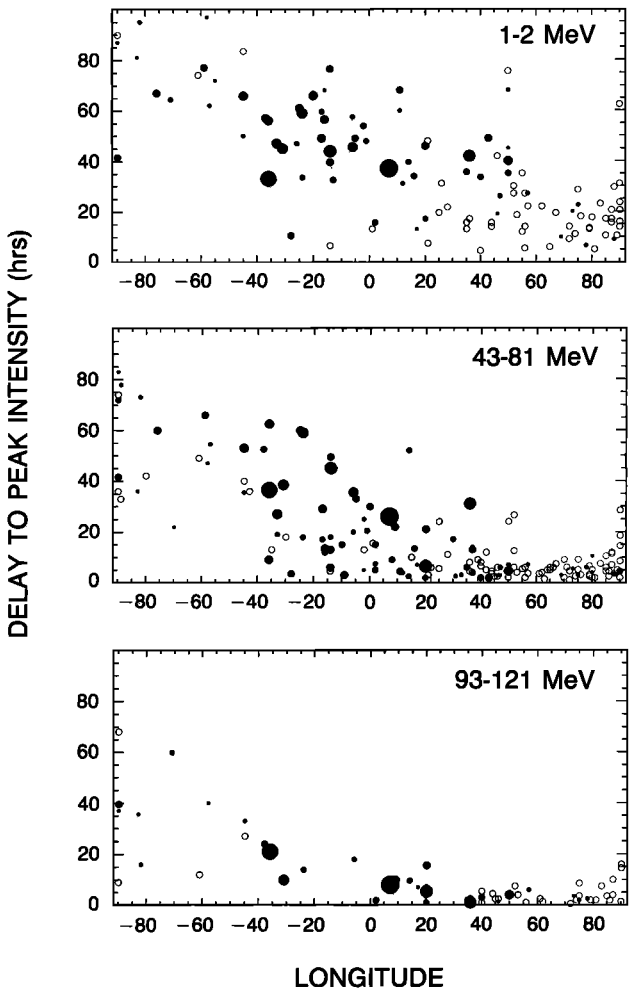

Fig. 8. Delays to peak intensities measured in hours for three different energy ranges (1–2, 43–81, and 93–121 MeV) as a function of the heliolongitudes of the associated flares. The open circles correspond to events which were not associated with shocks detected at Earth. The sizes of the solid circles are a measure of the strengths of the associated shocks.

relative contributions of solar and IP particles as a function of heliolongitude in a general way rather than for specific events.

Figure 8 shows delays as a function of heliolongitude for the energy ranges 1–2 MeV, 43–81 MeV, and 93–121 MeV. Open circles are used for events without associated shocks. For events associated with shocks the size of the circle is a measure of the shock strength which is based on the magnitude of the SC [see *Cane*, 1988].

Plots of delays as a function of heliolongitude formed the basis for the concept of "coronal propagation" [*Reinhard and Wibberenz*, 1974]. It was assumed that the long delays to maximum intensity for eastern events measured the time taken for the particles to diffuse across the solar disk, and the presence of IP shocks was not considered.

In Figure 9 we show the delays referenced to the shock passage. For the 9- to 23- and 43- to 81-MeV events we calculate the fractional time difference between the peak intensity and the shock passage for those events associated with a shock detected at Earth. The time difference is negative, zero, or positive if the particles peak after, at, or before shock passage. The time differences are normalized with respect to the shock transit time. Events which peak near the flare time have a difference close to 1. In the figure the size of the circles is a measure of the shock strength. The figures show that the delays are ordered with respect to heliolongitude and shock strength. Many events further east than about E30° peak after the shock has passed. The contribution of the IP shock component to the peak flux decreases the further west the source region and is less pronounced at the higher energy. However, if the shock is sufficiently strong, the intensities peak at the shock even at the higher energy, as may be seen in Figure 9 (bottom).

Figures 10 and 11 show how peak intensities vary as a function of heliolongitude and energy. The energy band for each figure is indicated. Note that for some 1- to 2-MeV events near central meridian the values are only approximate, as the detector saturates at intensities above about 10^4 particles cm^{-2} sr^{-1} s^{-1} MeV^{-1}. In the figures the solid circles are for events associated with IP shocks, with the strength of the shock indicated by the size of the circle. Open circles are used for events without associated shocks. Note that these events originate mainly in western regions and that the distribution

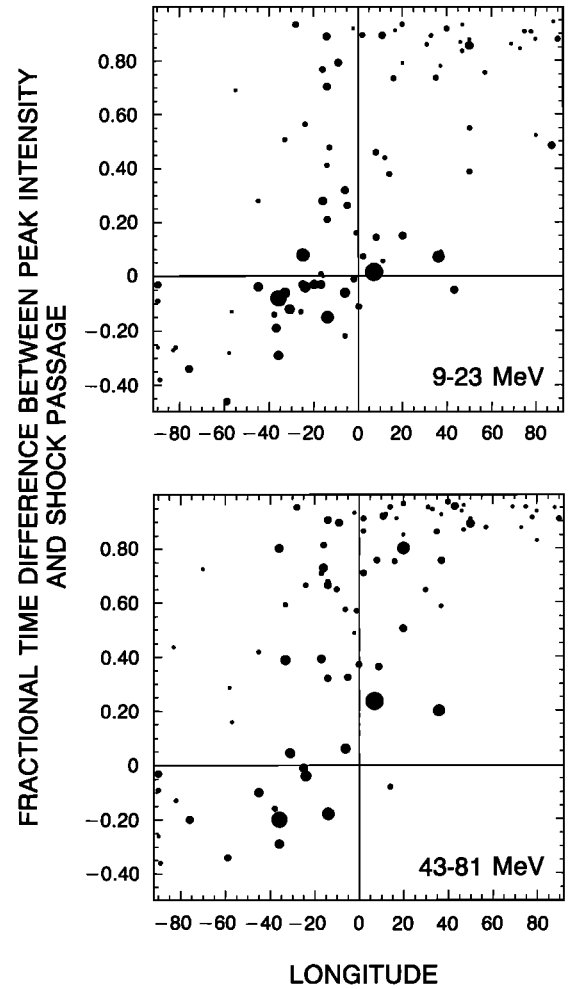

Fig. 9. Normalized time difference between the peak intensities and the passages of associated shocks as a function of the heliolongitudes of the associated flares. (For each event the time difference has been divided by the time for the associated shock to transit from the Sun to the Earth. Events which peak at the shock have a difference of 0, whereas events that peak soon after the flare have a difference of almost 1.) The sizes of the circles are a measure of the strengths of the associated shocks.

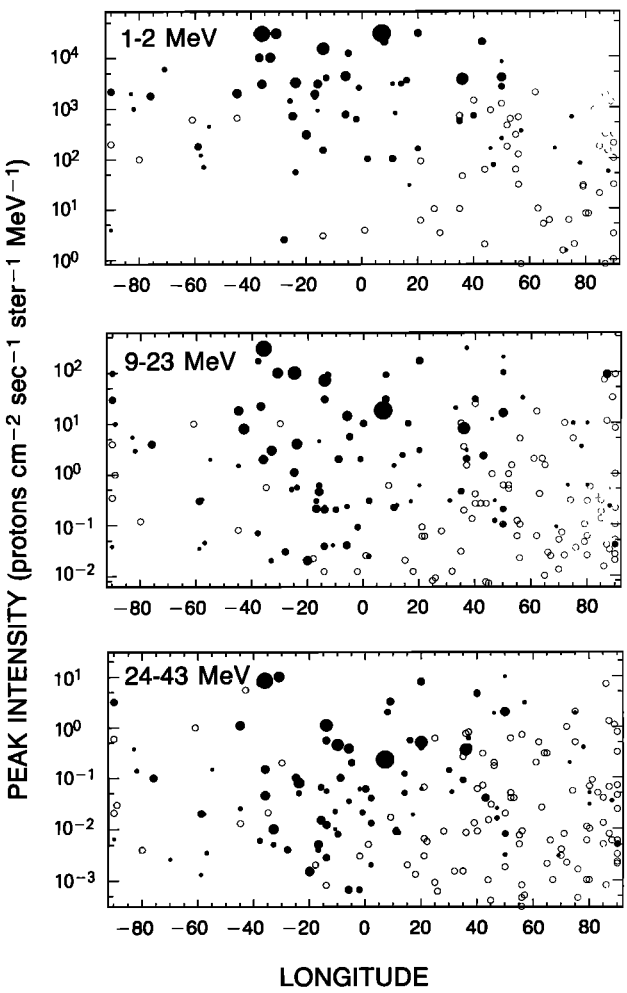

Fig. 10. Energy bands from 1 to 43 MeV.

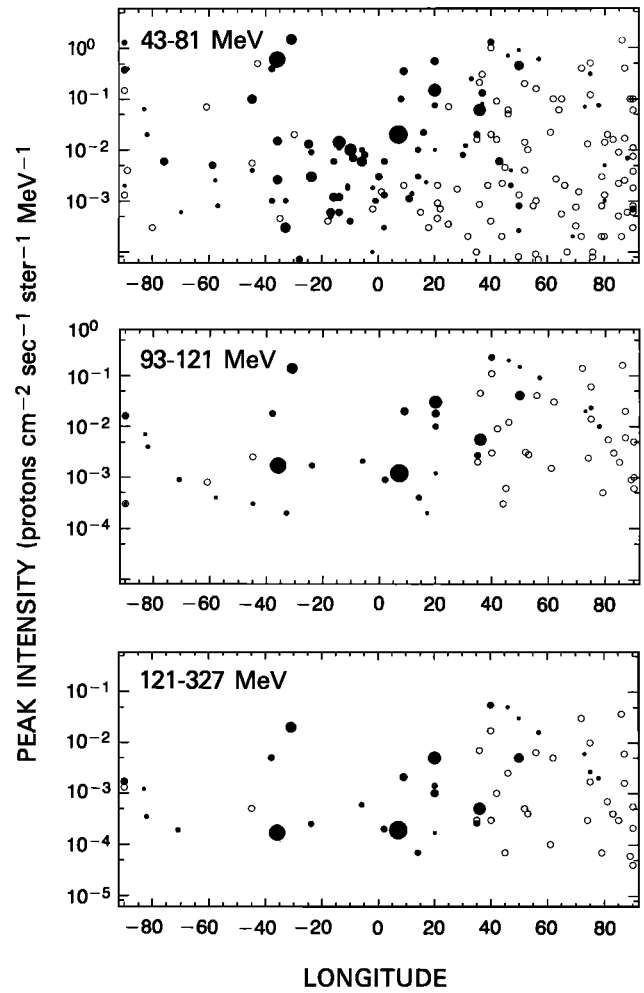

Fig. 11. Energy bands from 43 to 327 MeV.

Figures 10 and 11. Peak intensities, in six energy bands, as a function of the source regions. The open circles correspond to events which were not associated with shocks detected at Earth. The sizes of the filled circles are a measure of the strength of the associated shocks.

of their intensities provides some estimate of the decrease in amplitude of solar particles as a function of longitude.

It might be expected that individual large events would show longitudinal variations not unlike the upper envelopes of the intensities. In general, the highest intensities should be seen when the observer is well connected to the flare site. For particularly strong shocks it is possible that an observer to the west may see intensities associated with the shock which are higher than solar particle intensities seen by the well-connected observer. In fact, there is an example of this occurrence. In April of 1969 there were five widely spaced spacecraft all at about 1 AU from the sun. On April 10 there was a flare on the east limb, as viewed from Earth, which was associated with a huge interplanetary shock detected at each of the spacecraft [*Pinter*, 1977]. Thus the shock extended over 180° in longitude. Particle data at 8–45 MeV have been presented by *Reinhard and Wibberenz* [1974] and *Reinhard et al.* [1986], and it may be seen in their figures (Figure 10 and 1, respectively) that the highest intensities were seen by the spacecraft for which the flare was at E60°. The peak intensity, which was delayed, was almost an order of magnitude higher than that seen by the spacecraft which were well connected. Similarly, other single events viewed from different locations show the behavior we predict based on the single location analysis. Figure 12 shows sketches based on the observations presented by *McKibben* [1972]. Note that the increase on July 8 for the spacecraft viewing at E89° is seen by us as being part of the July 6 event. *McKibben* [1972] viewed it as another flare event but comments on the difficulty with this association.

Figure 13 shows an event observed by our experiments on IMP 8 and Helios 1 and 2 during March 1979. At this time the Helios 1 and 2 spacecraft were at about 0.9 AU and approximately 70° and 30°, respectively, to the east of the Earth-Sun line. Times of shock passages at the Helios spacecraft were obtained from the listing presented by *Volkmer and Neubauer* [1985]. Note that a subset of the March 1979 particle data (at a lower energy) was presented by *McGuire et al.* [1983]. In that paper, no consideration was taken of the presence of IP shocks. From a preliminary study of the data used by McGuire et al. and consideration of other multiple spacecraft studies we find that the events observed at widely separated spacecraft are associated with IP shocks.

Figure 14 shows the variation of the spectral index as a function of heliolongitude, assuming a power law for the in-

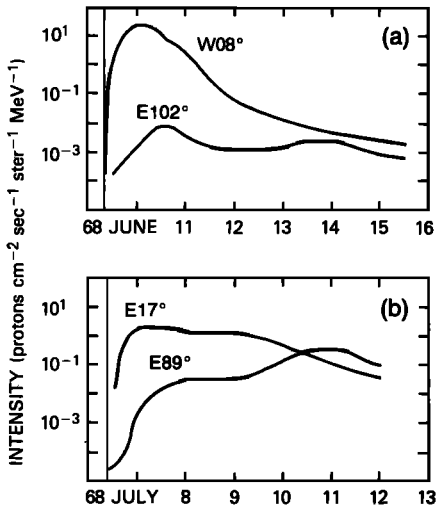

Fig. 12. Two events in June/July 1968 detected by three spacecraft (Pioneers 6 and 7 and IMP 4), all near 1 AU but at different elongations. The profiles are sketches of 15- to 18.7-MeV data presented by *McKibben* [1972]. (*a*) A flare on June 9 occurred at W08° relative to Earth and IMP 4. Relative to P 6 the flare was located at E102°. Relative to P 7 it was located at W76°. Shown are the P 6 and IMP 4 profiles. The P 7 profile was similar to the IMP 4 profile but had a smaller peak intensity. (*b*) A flare on July 6 occurred at E89°. The IMP 4 profile looks like ones shown in Figure 7. For P 6 the flare was located at E17°, and the profile is similar to Figure 5*a*. For P 7 the flare was at W114°. The profile was similar to the P 6 one but had lower intensity after July 8.

tensities between the two energy bands 23–43 and 43–81 MeV. Figure 14 should be compared with Figure 10 of *Van Hollebeke et al.* [1975]. One sees the same general features, namely. that most of the western and far eastern events have values in the range -2 to -4 and the majority of the steeper events originate near central meridian. By referring to Figure 14 one sees that the events with steeper spectra correspond to those with strong shocks. From the earliest studies it was known that ESP or delayed events had steep spectra [*Datlowe*, 1972]. Note that the spectral index is a measure of the relative contributions of the solar and IP particles. The steep spectrum means that at low energies there are a lot of locally accelerated particles.

3. Discussion

The shape of a particle increase is, to a large extent, determined by the longitude of the solar event relative to the observer and, in particular, to the presence and the strength of an associated shock. We believe that the presence of an interplanetary shock determines whether a far eastern event will be seen at all. These assertions are based primarily on the study of a large sample of individual events detected at Earth but are supported by observations of isolated events from spacecraft at different locations.

Assuming that high-energy particles are accelerated by shocks, one can explain the characteristics of events as a function of heliolongitude in terms of the large-scale structure of IP shocks. The schematic presented in a recent paper by *Cane* [1988] is shown in Figure 15. The most important point to note is the change in shock strength as a function of heliolongitude. The highest compression occurs in a region near the nose of the shock but centered about 15° toward the western flank. Another important point is the presence of the ejected coronal material, the shock driver. There have been several different phenomena identified as shock drivers, one of which is the bidirectional streaming of low-energy protons [e.g., *Marsden et al.*, 1987; *Sanderson et al.*, 1983].

In order to relate the observed particle profiles to the large-scale structure of interplanetary shocks we consider the consequences of intercepting a shock at positions indicated by A, B, C, and D in Figure 15. In the figure we show 20-MeV profiles of actual events which are representative of events from the appropriate heliolongitudes. The profiles should be compared with those detected by different spacecraft for the same event as presented in Figure 13. Note that a shock originating in a western region will be intercepted on its eastern flank. It is easiest to understand the profiles if one considers the shock to be stationary and the spacecraft to be moving. For each effective path of a spacecraft we would expect the following:

Path A

Path A encounters the nose of the shock where the compression is greatest. At the energy shown, the overall peak of the event results from particles accelerated in the solar corona. The IP shock-accelerated particles are relatively weak in com-

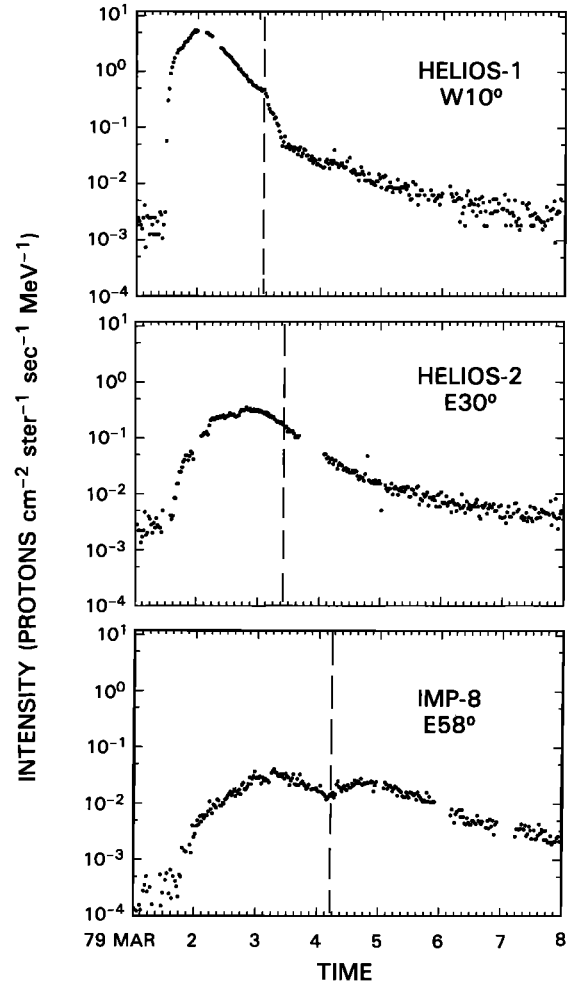

Fig. 13. Intensities detected at IMP 8 and Helios 1 and 2 during March 1979. The Helios spacecraft were located at about 0.9 AU and at about 70° and 30° east of the Earth-Sun line. There was a flare on March 1 at E58° relative to Earth. The locations relative to the Helios spacecraft are listed on the figure. Shock passages at the spacecraft are indicated by dashed lines. The energy band for the Helios spacecraft was 20–30 MeV. For the IMP 8 data we show the energy band 24–29 MeV.

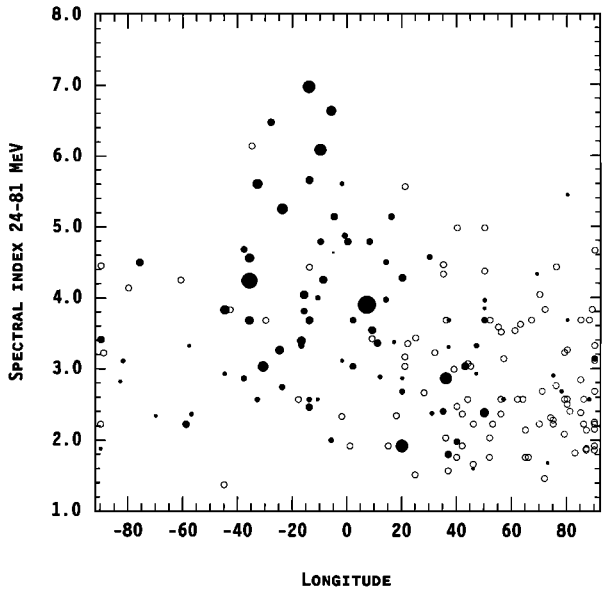

Fig. 14. Power law energy spectral indices in the range 20–40 MeV. Open circles are for events not associated with shocks detected at Earth. Note that the steep spectra occur near central meridian for the strongest shocks.

parison. They maximize in the compressed region behind the shock. Subsequently, the intensities drop rapidly as the spacecraft enters the driver gas. As the spacecraft leaves the driver, the intensities increase briefly before beginning a slow decline.

Path B

Path B encounters the shock in a region of high compression but does not encounter the driver. Behind the shock the spacecraft remains connected to the region of high compression for a long time. Consequently, the spacecraft resides in magnetic intensity tubes between the sun and the shock that have been filled with particles accelerated for several days. The profile is dominated by shock-accelerated particles.

Path C

If the shock is very energetic, this path will detect a profile much like that of B, although more drawn out. The spacecraft will remain connected to the shock for a longer time. In addition, the western flank travels a little more slowly than the nose of the shock. For a less energetic shock the highest intensities will occur well behind the shock. In some cases the spacecraft will not detect the shock.

Path D

For this path the shock is encountered in a region where shocks are usually weak. The particle profile is dominated by solar particles which travel directly to the spacecraft at the onset of the solar event. After passing through the shock the spacecraft becomes more poorly connected to the shock.

With Figure 15 we primarily address the shape of the intensity profiles, but the relative intensities are approximately what one might expect (cf. Figure 13). At energies above 20 MeV one expects that the highest intensities will be due to prompt solar particles, i.e., path D will see the highest intensities. At energies below about 10 MeV the shock-accelerated particles have higher intensities than the solar particles. At these energies the particles do not travel away from the shock as easily as do higher-energy particles. The highest intensities occur where the shock is strongest and are thus seen at these energies for path A.

In Figure 15 we show that at 20 MeV, path B has the

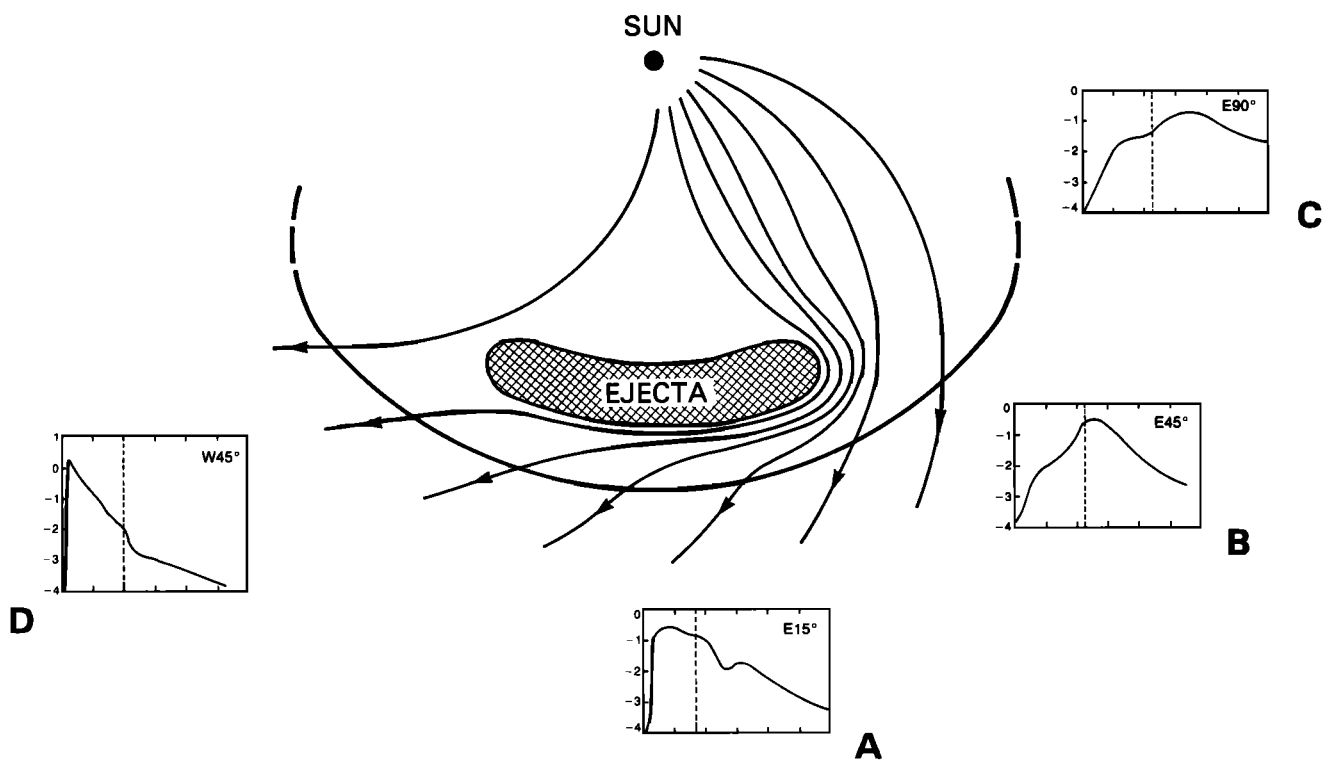

Fig. 15. The figure shows representative profiles of actual events at 20 MeV for different spacecraft trajectories through a shock. Note that for a very energetic shock the western flank would be more extensive than the picture presented here. See the text for a more detailed description of this figure.

highest shock-associated intensities. Figure 11 shows that events near E30° have higher peak intensities than those nearer central meridian. From the delays we find that a switch to higher intensities occurs when the events switch to peaking behind the shock. It seems possible that the "hole" near central meridian seen in Figure 11 is a real effect and results from the absence of postshock particles after the spacecraft enters the driver and becomes disconnected from the shock.

We have provided evidence that IP shocks are associated with the majority of high-energy, high-intensity proton events and that these shocks play a dominant role in determining the intensity time structure of an event. We now address the mechanism by which the shocks accelerate particles. Crucial to arguments about the mechanism is the geometry of the shocks, i.e., the angle between the shock normal and the upstream magnetic field. Are the shocks parallel, oblique, or perpendicular? This question was addressed by *Cane* [1988], and it was concluded (see Figure 15) that for the most part the shock surfaces would form oblique shocks. Perpendicular shocks are unlikely to be involved. In some previous studies of ESP events [e.g., *Sarris et al.*, 1984; *Sarris et al.*, 1985] the large-scale shock structure sketched by *Hundhausen* [1972] was assumed. In this picture the shock is tightly coupled to the driver, and consequently, the western flanks of shocks would be expected to be perpendicular. However, *Cane* [1988] has presented data which suggest that for the most energetic shocks, which are the ones which generate ESP events, the Hundhausen picture is not correct.

Perpendicular shocks might exist on the extreme western flanks, detected for east limb flares, but it seems likely that for east limb events the particles are probably accelerated at the part of the shock where it is oblique. That the shocks are not perpendicular as measured in situ has been established for some of the events of our study. A number of the class A and B events discussed by *van Nes et al.* [1984] are the low-energy counterparts of events of our study. The normals of the associated shocks had median values of 47° and 66°. None of the van Nes et al. class C events are common to our study. The shocks associated with this class had a medium shock normal of 75°. Thus, given the choices usually discussed in the literature, i.e., shock drift versus diffusive, the most likely mechanism is diffusive acceleration. This mechanism has been shown to operate at low energies [*van Nes et al.*, 1984]. Further support for a diffusive acceleration process is the observation that the shock effects are more apparent as shock compressions increase.

The question of particle acceleration and propagation in the corona is best addressed by high time resolution data obtained in the first few hours of event onsets where IP shock effects are minimal. From the present study it is clear that studies [e.g., *Reinhard and Wibberenz*, 1974] based on the very long delays to maximum intensity for eastern events do not provide information about processes in the corona. Such data sets (and also those of *Van Hollebeke et al* [1975]) are dominated by IP shock effects.

4. CONCLUSIONS

Proton increases have well-defined forms dependent on the location of the source relative to the observer and the presence and strength of associated interplanetary shocks. This consistency of behavior arises because of the dominant role of interplanetary shocks and has been illustrated with many examples of intensity-time profiles and a statistical analysis of several hundred events occurring over almost two solar cycles. The assertion that proton increases have this predictable behavior is supported by multiple spacecraft observations.

Solar particle events are composed of a solar component and often a shock component. Coronal processes are not discussed in this paper except to show that coronal processes are not responsible for the long delays to maximum intensity in eastern events.

Knowledge of the large-scale structure of interplanetary shocks has enabled us to explain the change in shock effects as a function of longitude and energy. Shocks are strongest when observed along the radial from the source region. Thus the highest shock-associated intensities are generally observed from central meridian flares. For shocks detected on their western flanks the highest intensities generally occur when the shock is beyond the observer, since there is then a connection to the nose of the shock. Shocks detected on their eastern flanks are usually weak and produce small effects.

Acknowledgments. The authors wish to thank Sito Balleza for carefully compiling a large part of the data base for the statistical study. We also thank Bob McGuire for assistance in transferring the Goddard Space Flight Center (GSFC) data sets to PCs. This work was supported at GSFC/University of Maryland under grant NGR 21-002316.

The Editor thanks G. Wibberenz and another referee for their assistance in evaluating this paper.

REFERENCES

Bame, S. J., J. R. Ashbridge, W. C. Feldman, J. T. Gosling, and R. D. Zwickl, Bi-directional streaming of solar wind electrons >80 eV: ISEE evidence for a closed field structure within the driver gas of an interplanetary shock, *Geophys. Res. Lett.*, *8*, 173, 1981.

Beeck, J., G. M. Mason, D. C. Hamilton, G. Wibberenz, H. Kunow, D. Hovestadt, and B. Klecker, *Astrophys. J.*, *322*, 1052, 1987.

Bryant, D. A., T. L. Cline, U. D. Desai, and F. B. McDonald, Explorer 12 observations of solar cosmic rays and energetic storm particles after the solar flare of September 28, 1961, *J. Geophys. Res.*, *67*, 4983, 1962.

Burlaga, L., E. Sittler, F. Mariani, and R. Schwenn, Magnetic loop behind an interplanetary shock: Voyager, Helios and Imp 8 observations, *J. Geophys. Res.*, *86*, 6673, 1981.

Cane, H. V., The evolution of interplanetary shocks, *J. Geophys. Res.*, *90*, 191, 1985.

Cane, H. V., The large-scale structure of flare-associated interplanetary shocks, *J. Geophys. Res.*, *93*, 1, 1988.

Cane, H. V., R. E. McGuire, and T. T. von Rosenvinge, Two classes of solar energetic particle events associated with impulsive and long-duration soft X-ray flares, *Astrophys. J.*, *301*, 448, 1986.

Cane, H. V., D. V. Reames, and T. T. von Rosenvinge, On the sources of solar energetic proton events, *Conf. Pap. Int. Cosmic Ray Conf.*, *20*, 217, 1987.

Datlowe, D., Association between interplanetary shock waves and delayed solar particle events, *J. Geophys. Res.*, *77*, 5374, 1972.

Evenson, P. A., P. Meyer, and S. Yanagita, Solar flare shocks in interplanetary space and solar flare particle events, *J. Geophys. Res.*, *87*, 625, 1982.

Gosling, J. T., D. N. Baker, S. J. Bame, W. C. Feldman, R. D. Zwickl, and E. J. Smith, Bidirectional solar wind electron heat flux events, *J. Geophys. Res.*, *92*, 8519, 1987.

Hundhausen, A. J., *Coronal Expansion and Solar Wind*, Springer-Verlag, New York, 1972.

Kahler, S. W., The role of the big flare syndrome in correlations of solar energetic proton fluxes and associated microwave burst parameters, *J. Geophys. Res.*, *87*, 3439, 1982.

Kennel, C. F., F. V. Coroniti, F. L. Scarf, W. A. Livesay, C. T. Russell, E. J. Smith, K.-P. Wenzel, and M. Scholer, A test of Lee's quasi-linear theory of ion acceleration by interplanetary travelling shocks, *J. Geophys. Res.*, *91*, 11917, 1986.

Lee, M. A., Coupled hydromagnetic wave excitation and ion acceleration at interplanetary traveling shocks, *J. Geophys. Res.*, *99*, 6109, 1983.

Lee, M. A., and J. M. Ryan, Time-dependent coronal shock acceleration of energetic solar flare particles, *Astrophys. J., 303*, 829, 1986.

Marsden, R. G., T. R. Sanderson, C. Tranquille, K.-P. Wenzel, and E. J. Smith, ISEE-3 observations of low energy proton bidirectional events and their relation to transient interplanetary magnetic structures, *J. Geophys. Res., 92*, 11009, 1987.

McGuire, R. E., M. A. I. Van Hollebeke, and N. Lal, A multispacecraft study of the coronal and interplanetary transport of solar cosmic rays, *Conf. Pap. Int. Cosmic Ray Conf., 18*, 353, 1983.

McKibben, R. B., Azimuthal propagation of low-energy solar-flare protons as observed from spacecraft very widely separated in solar azimuth, *J. Geophys. Res., 77*, 3957, 1972.

Parker, E. N., *Interplanetary Dynamical Processes*, Wiley-Interscience, New York, 1963.

Pinter, S., Directional properties of the propagation of solar flare-generated shock waves in interplanetary space, Study of Travelling Interplanetary Phenomena, *AFGL-TR-77-0309*, edited by M. A. Shea, D. F. Smart and S. T. Wu, p. 161, Air Force Geophys. Lab., Bedford, Mass., 1977.

Reames, D. V., and R. G. Stone, The identification of solar ^{3}He-rich events and the study of particle acceleration at the sun, *Astrophys. J., 308*, 902, 1986.

Reinhard, R., and G. Wibberenz, Propagation of flare protons in the solar atmosphere, *Sol. Phys., 36*, 473, 1974.

Reinhard, R., E. C. Roelof, and R. E. Gold, Separation and analysis of temporal and spatial variations in the 10 April 1969 solar flare particle event, in *The Sun and Heliosphere in Three Dimensions*, edited by R. Marsden, D. Reidel, Hingham, Mass., 1986.

Richter, A. K., M. I. Verigin, V. G. Kurt, V. G. Stolpovsky, K. I. Gringauz, E. Keppler, H. Rosenbauer, M. Neubauer, T. Gombosi, and A. Somogyi, The January 1978 interplanetary shock event as observed by energetic particles, plasma and magnetic field devices on board of Helios-1, Helios-2 and Prognoz-6, *J. Geophys., 50*, 101, 1981.

Sanderson, T. R., R. Reinhard, and K.-P. Wenzel, The propagation of upstream protons between the earth's bow shock and ISEE-3, *J. Geophys. Res., 86*, 4425, 1981.

Sanderson, T. R., R. G. Marsden, R. Reinhard, K.-P. Wenzel, and E. J. Smith, Correlated particle and magnetic field observations of a large-scale loop structure behind an interplanetary shock, *Geophys. Res. Lett., 10*, 916, 1983.

Sarris, E. T., G. C. Anagnostopoulos, and P. C. Trochoutsos, On the E-W asymmetry and the generation of ESP events, *Sol. Phys., 93*, 195, 1984.

Sarris, E. T., R. B. Decker, and S. M. Krimigis, Deep space observations of the east-west asymmetry of solar energetic particle events: Voyagers 1 and 2, *J. Geophys. Res., 90*, 3961, 1985.

Scholer, M., and G. Morfill, Simulation of solar flare particle interaction with interplanetary shock waves, *Sol. Phys., 45*, 227, 1975.

Van Hollebeke, M. A. I., L. S. Ma Sung, and F. B. McDonald, The variation of solar proton energy spectra and size distribution with heliolongitude, *Sol. Phys., 41*, 189, 1975.

van Nes, P., R. Reinhard, T. R. Sanderson, K.-P. Wenzel, and R. D. Zwickl, The energy spectrum of 35-1600 keV protons associated with interplanetary shocks, *J. Geophys. Res., 89*, 2122, 1984.

Volkmer, P. M., F. M. Neubauer, Statistical properties of fast magnetoacoustic shock waves in the solar wind between 0.3 AU and 1 AU: Helios-1, 2 observations, *Ann. Geophys., 3*, 1, 1985.

Wibberenz, G., L. J. Lanzerotti, and D. Venkatesan, Solar particle propagation in the interplanetary environment: A study of the November 18, 1968, event, *J. Geophys. Res., 81*, 5807, 1976.

H. V. Cane, D. V. Reames, and T. T. von Rosenvinge, NASA Goddard Space Flight Center, Code 661, Greenbelt, MD 20771.

(Received January 15, 1988;
revised April 14, 1988;
accepted May 3, 1988.)